ISSN 1070-4280, Russian Journal of Organic Chemistry, 2016, Vol. 52, No. 10, pp. 1503–1508. © Pleiades Publishing, Ltd., 2016.
Original Russian Text © E.N. Ovchenkova, N.G. Bichan, T.N. Lomova, 2016, published in Zhurnal Organicheskoi Khimii, 2016, Vol. 52, No. 10, pp. 1509–1515.

Synthesis and Properties of a New (Octaethylporphyrinato)-manganese(III)–Pyridinyl-Substituted Pyrrolidinofullerene Dyad

E. N. Ovchenkova, N. G. Bichan, and T. N. Lomova*

Krestov Institute of Solution Chemistry, Russian Academy of Sciences, ul. Akademicheskaya 1, Ivanovo, 153045 Russia
**e-mail: tnl@isc-ras.ru*

Received April 25, 2016

Abstract—The formation of a porphyrin–fullerene dyad from 2′-(pyridin-4-yl)-5′-(pyridin-2-yl)-1′-(pyridin-3-ylmethyl)-2′,5′-dihydro-1′*H*-pyrrolo[3′,4′:1,9](C_{60}-I_h)[5,6]fullerene and (2,3,7,8,12,13,17,18-octaethylporphyrinato)manganese(III) with axial chloride ligand has been studied on a quantitative level with the goal of obtaining supramolecules possessing biological activity. Preliminarily, the reaction of manganese(III) porphyrin with pyridine has been studied. The donor–acceptor dyads are formed either instantaneously and reversibly (pyridine) or slowly and irreversibly (substituted fullerene). In both cases, the reaction is a one-step process for which thermodynamic and kinetic parameters have been determined. The results can be used to optimize conditions for the synthesis of porphyrin–fullerene dyads. The obtained dyads have been characterized by spectral data and stability constants.

DOI: 10.1134/S1070428016100213

Resistance of infectious agents to antibiotics and inability of pharmaceutical industry to create new antibiotic strains are growing problems in health protection [1, 2]. Nowadays, considerable attention is given to the synthesis of new antibacterial agents [3–6]. Among the latter, of particular interest are porphyrin complexes [7–9] due to their ability to act as photosensitizers. Antimicrobial photodynamic therapy, i.e. photodynamic inactivation of microorganism, is a new alternative method for the treatment of microbial infections [10–12].

Interest in manganese porphyrins that are subjects of the present study is determined by biological importance of manganese. Manganese is necessary for normal physiological development of living organisms. The role of manganese in functioning of such enzymes as superoxide dismutase, glutamine synthetase, and arginase has been revealed [13]. Antibacterial properties of manganese(III) tetraphenylporphyrin against gram positive *Staphylococcus aureus* have been reported [14]. Manganese(III) complexes with porphyrins containing 4-aminophenyl and *N*-phenylureido groups in the *meso* positions show considerably higher antibacterial and antifungal activity than their unsubstituted analogs against gram negative *Escherichia coli* and *Pseudomonas aeruginosa*, gram positive *Bacillus subtilis*, *Aspergillus oryzae*, and *Candida albicans* [15]. At present, not only porphyrins and their metal complexes but also supramolecular systems based thereon with additional pharmacophoric fragments are

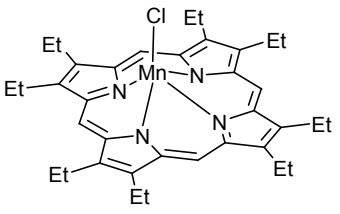

(Cl)MnOEtPor

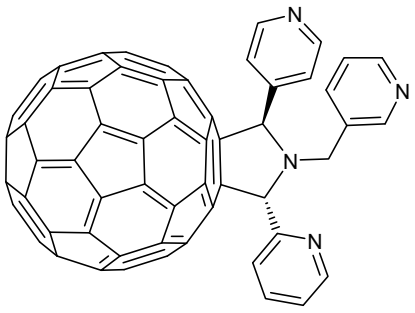

Py_3C_{60}

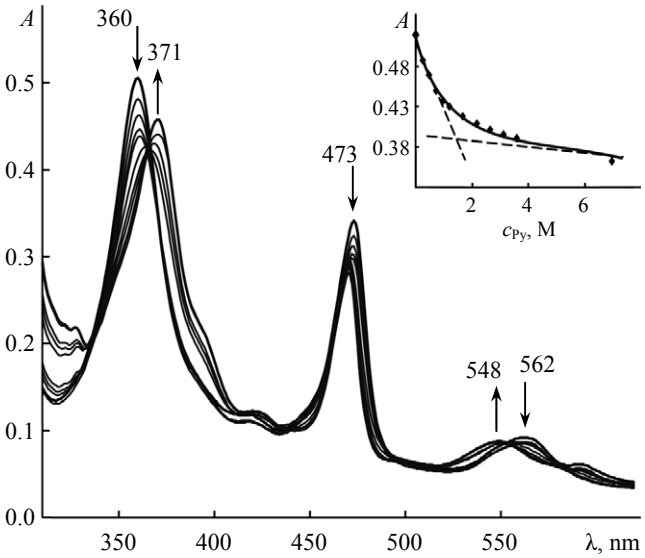

Fig. 1. Variation of the electronic absorption spectrum of (Cl)MnOEtPor in toluene upon addition of pyridine (0 to 7 M). The insert shows the spectrophotometric titration curve at λ 360 nm.

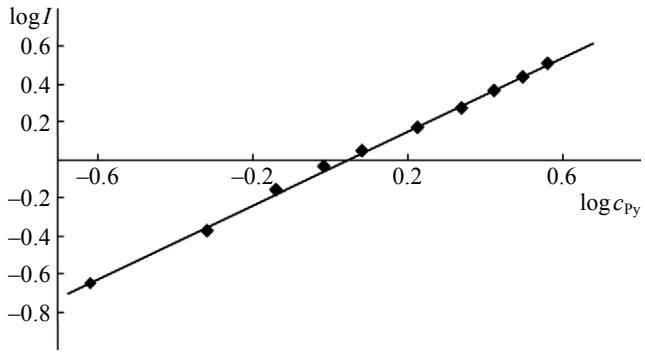

Fig. 2. Logarithmic dependence of I on the pyridine concentration c_{Py} for the reaction of (Cl)MnOEtPor with pyridine at 298 K; $\tan\alpha = 0.98$ ($R^2 = 0.99$).

extensively studied. For example, the activity of fullerene systems against *E. coli* and herpes viruses, including cytomegalovirus, has been reported [16, 17].

We have synthesized supramolecular systems from (chloro)(2,3,7,8,12,13,17,18-octaethylporphyrinato)-manganese(III) [(Cl)MnOEtPor] and an organic base, 2′-(pyridin-4-yl)-5′-(pyridin-2-yl)-1′-(pyridin-3-ylmethyl)-2′,5′-dihydro-1′*H*-pyrrolo[3′,4′:1,9](C_{60}-I_h)-[5,6]fullerene (Py_3C_{60}) and characterized them by physicochemical methods. Taking into account that Py_3C_{60} binds to manganese(III) through pyridine residues, it was necessary to study the reaction of (Cl)MnOEtPor with pyridine. The equilibrium in this system was achieved immediately after mixing the reactants; the electronic spectra showed changes of the position and intensity of the main absorption maxima of (Cl)MnOEtPor with retention of isosbestic points. The Soret band shifted red by 11 nm, the charge-transfer band ($\pi \rightarrow d$ transition) shifted blue by 2 nm, and the blue shift of the Q band was 14 nm (Fig. 1). The spectrophotometric titration curve was a straight line with a bent at the minimum optical density, which corresponds to a one-step process. Figure 1 shows the transition area.

The slope of the logarithmic dependence of I versus c_{Py} (Fig. 2) is close to unity, which suggests 1 : 1 complex formation; $K = 0.90 \pm 0.03$ L/mol (Scheme 1). The product is a donor–acceptor complex of pyridine with (Cl)MnOEtPor (see below).

Scheme 1.

$$\text{(Cl)MnOEtPor} + \text{Py} \underset{}{\overset{K}{\rightleftharpoons}} \text{(Cl)(Py)(MnOEtPor)}$$

The spectrophotometric titration data for the reaction of (Cl)MnOEtPor with pyridine (Fig. 1) suggest axial coordination of pyridine molecule to Mn(III) without elimination of the chloride ion. This coordination mode reduces deviation of the manganese atom from the porphyrin macrocycle plane and is responsible for the blue shift of the Q band in the electronic absorption spectrum. The observed spectral variations are consistent with published data. According to [18], addition of pyridine to a benzene solution of (acetoxo)-(2,8,12,18-tetrabutyl-3,7,13,17-tetramethyl-5,15-diphenylporphyrinato)manganese(III) induces a blue shift of the charge-transfer band.

The product structure was also optimized by PM3 quantum chemical simulation of (Cl)MnOEtPor and pyridine molecules and the corresponding 1 : 1 donor–acceptor dyad. The latter was calculated with different mutual orientations of the chloride ion and pyridine molecule. Figure 3 shows the optimized structures of (Cl)MnOEtPor and complexes (Cl)(Py)MnOEtPor (heats of formation –110.03 and –46.01 kcal/mol) with *trans* and *cis* orientations of the chloride ion with respect to the pyridine molecule. The complex with *trans* orientation of the axial ligands (Fig. 3, b) was characterized by the lowest heat of formation and was assumed to be the most probable. The calculations showed that the manganese atom in the complex (Cl)(Py)MnOEtPor deviates from the plane formed by the porphyrin nitrogen atoms (N_4) by 0.75 Å and that the corresponding deviation in *trans*-(Cl)(Py)MnOEtPor is 0.26 Å.

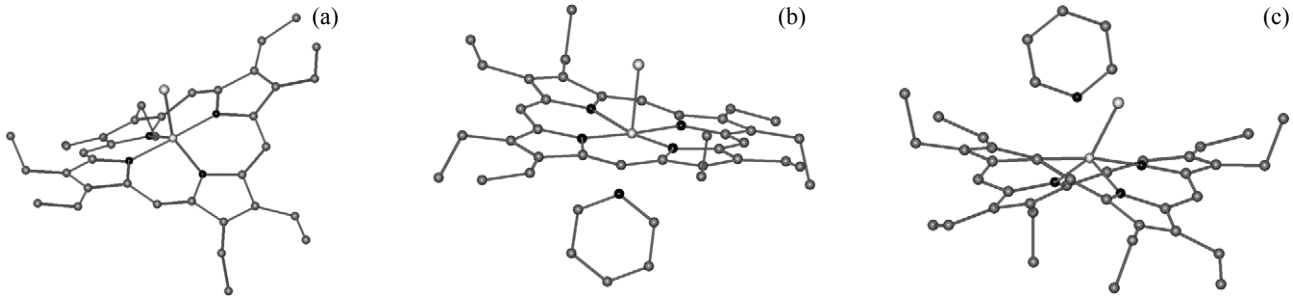

Fig. 3. Optimized (PM3) structures of (a) (Cl)MnOEtPor and its complexes with pyridine with (b) *trans* and (c) *cis* orientations of the axial ligands.

The formation of (Cl)(Py)MnOEtPor was also monitored by variation of characteristic IR absorption bands of the porphyrin macrocycle. Appreciable changes, in particular a high-frequency shift by 4–6 cm^{-1}, were observed in the region 1600–1640 cm^{-1} typical of skeletal vibrations. This shift may be rationalized by movement of the manganese atom toward the macrocycle plane. It is known that skeletal vibration frequencies of porphyrins are sensitive to chemical modifications such as functional substitution and axial coordination [19]. The C–H stretching frequencies of the ethyl groups change only slightly upon formation of (Cl)(Py)MnOEtPor. The IR spectrum of (Cl)(Py)MnOEtPor contained new bands at 1741, 1702, 1405, 1220, 1180, 922, 876, 716, 702, and 398 cm^{-1} due to vibrations of N-bonded pyridine [20]; no such bands were observed in the spectrum of (Cl)MnOEtPor. The vibrational frequencies of coordinated pyridine were higher by ~5–35 cm^{-1} than those in the spectrum of free pyridine. A new weak band at 468 cm^{-1} in the spectrum of (Cl)(Py)MnOEtPor was assigned to the Mn–N_{Py} bond [19].

Analogous spectral variations were observed for the reaction of (Cl)MnOEtPor with Py_3C_{60}, but some time was necessary for equilibration. The electronic absorption spectrum of a mixture of (Cl)MnOEtPor and Py_3C_{60} in toluene showed gradual decrease of the absorption intensity at λ_{max} 473 nm and increase of the absorbance at λ_{max} 468 nm with a distinct isosbestic point (Fig. 4). The electronic absorption spectrum of the product corresponds to the manganese(III) porphyrin chromophore. As we showed previously [21] by Beer–Lambert measurements, neither aggregation nor other processes were observed in the system Py_3C_{60}–toluene in the absence of metal porphyrin.

Effective rate constants k_{ef} of the reaction of (Cl)MnOEtPor with Py_3C_{60} in toluene at 298 K

Py_3C_{60} concentration, 10^{-5} M	$k_{ef}\times10^5$, s^{-1}	$k\times10^2$, L mol^{-1} s^{-1}
4.92	0.59±0.06	4.04
9.84	1.15±0.12	4.23
12.80	1.34±0.11	3.91
15.70	1.70±0.11	4.13

By kinetic study of the reaction of (Cl)MnOEtPor with Py_3C_{60} at different concentrations of the latter we determined first orders of the reaction with respect to both reactants (Figs. 5, 6) and calculated effective first-order rate constants k_{ef} (see table) and bimolecular rate constants k [Eq. (1)].

$$-\partial c_{(Cl)MnOEtPor}/\partial\tau = k c_{(Cl)MnOEtPor} c_{Py_3C_{60}} = (4.07\pm0.14)\times10^{-2} c_{(Cl)MnOEtPor} c_{Py_3C_{60}}. \quad (1)$$

Thus, the kinetics of the reaction of (Cl)MnOEtPor with Py_3C_{60} corresponds to irreversible bimolecular reaction with the formation of 1 : 1 complex

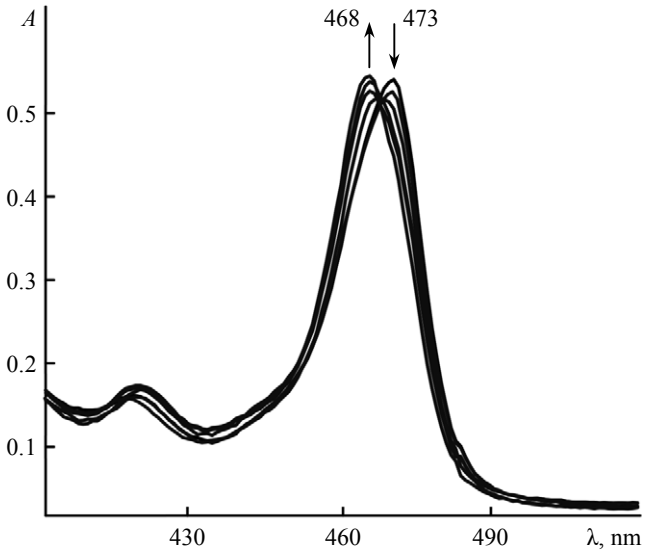

Fig. 4. Variation of the electronic absorption spectrum of (Cl)MnOEtPor in toluene containing Py_3C_{60} (c = 4.92×10^{-5} M) over 5 days.

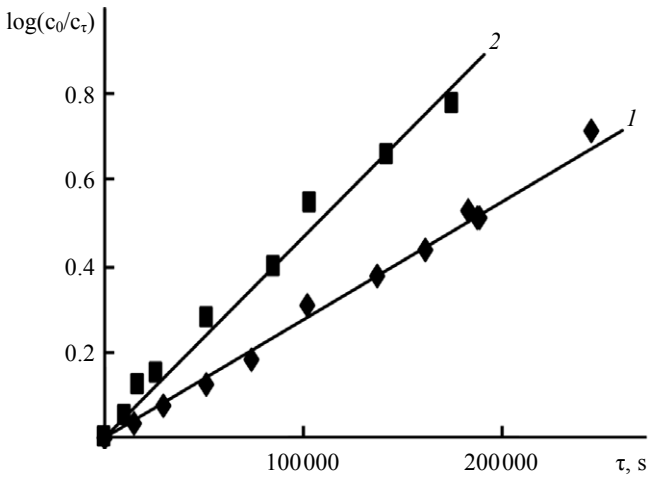

Fig. 5. Plot of $\ln(c_0/c_\tau)$ versus time τ for the reaction of (Cl)MnOEtPor with Py_3C_{60} in toluene. Concentration of Py_3C_{60}, M: (*1*) 4.92×10^{-5}, (*2*) 9.84×10^{-5}; $R^2 = 0.97$–0.99.

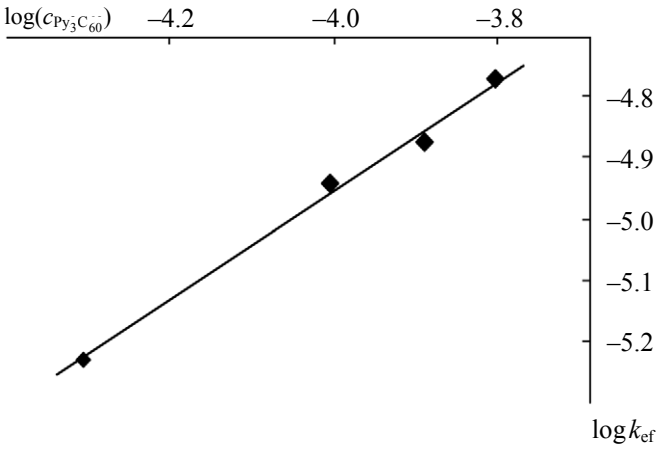

Fig. 6. Logarithmic dependence of k_{ef} on the Py_3C_{60} concentration for the reaction of (Cl)MnOEtPor with Py_3C_{60} in toluene; $\tan\alpha = 0.89$ ($R^2 = 0.99$).

(Cl)(Py_3C_{60})MnOEtPor whose structure is shown below. Such supramolecules are often called *coordination dyads* [22]. Analogous indium(III) porphyrin–fullerene coordination dyads were reported by us previously, and their structures were optimized by quantum chemical methods [23, 24].

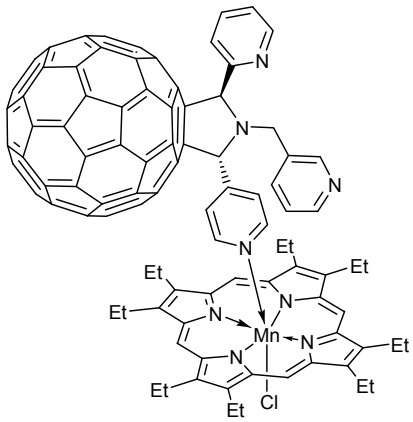

(Cl)(Py_3C_{60})MnOEtPor

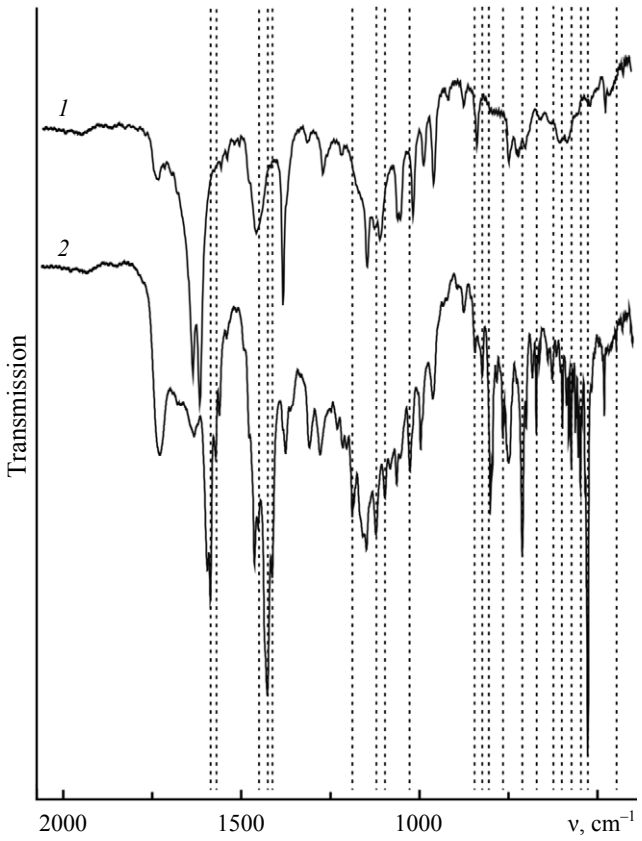

Fig. 7. IR spectra (KBr) of (*1*) (Cl)MnOEtPor and (*2*) (Cl)(Py_3C_{60})MnOEtPor. Dotted lines correspond to the vibrational frequencies of N-coordinated Py_3C_{60}.

The IR spectrum of (Cl)(Py_3C_{60})MnOEtPor in KBr (Fig. 7) displayed new bands at 1587, 1572, 1452, 1427, 1413, 1376, 1185, 1121, 1096, 1063, 1026, 876, 823, 800, 766, 711, 672, 628, 599, 574, 549, and 527 cm^{-1} due to N-coordinated Py_3C_{60}; these bands are lacking in the spectrum of (Cl)MnOEtPor. The bands at 1427, 1185, 574, and 527 cm^{-1} correspond to skeletal vibrations of C_{60} [25], and their position almost does not change in going from free Py_3C_{60} to the dyad. Vibrational frequencies typical of the pyridine and pyrrolidine rings of pure Py_3C_{60} increased by about 5–35 cm^{-1} (see Experimental). A new weak absorption band at 466 cm^{-1} is likely to belong to $Mn–N_{Py}$ stretchings [19].

We previously studied the reaction of Py_3C_{60} with (acetoxo)[oktakis(4-*tert*-butylphenyl)tetraazaporphyri-

nato]manganese(III) (AcO)MnTAP(4-*t*-BuPh)$_8$ in toluene [21], which afforded the corresponding coordination dyad, as in the reaction with (Cl)MnOEtPor. However, the reaction rate [$k = (2.5 \pm 0.26)\times10^{-8}$ L×mol^{-1} s^{-1}) was inversely proportional to the Py_3C_{60} concentration, and the rate-determining step was irreversible elimination of acetate ion from (AcO)(Py_3C_{60})–MnTAP(4-*t*-BuC_6H_4)$_8$. Thus, modification of tetrapyrrole macrocycle via aza or alkyl substitution sharply (by 6 orders of magnitude) slows down the formation of porphyrin–fullerene dyad and changes its composition. Our results may be used for optimization of the synthesis of porphyrin–fullerene dyads.

In summary, we have performed a quantitative study of the formation of coordination dyads from (chloro)(2,3,7,8,12,13,17,18-octaethylporphyrinato)-manganese(III) and organic bases, pyridine and pyridine-containing fullerene. The reaction kinetics in toluene were studied by spectrophotometry at 298 K. The reactants and products were identified by UV-Vis, IR, and mass spectra, and their structure was optimized by PM3 quantum-chemical calculations. Taking into account growing interest in new biologically active supramolecular systems based on macroheterocycles, the obtained results are promising for biomedical studies.

EXPERIMENTAL

The electronic absorption spectra were measured on an Agilent 8453 spectrophotometer. The IR spectra were recorded on a Bruker Vertex 80v spectrometer. The mass spectra were obtained on a Bruker Autoflex instrument.

(Chloro)(2,3,7,8,12,13,17,18-octaethylporphyrinato)manganese(III) [(Cl)MnOEtPor] was synthesized by reaction of manganese(II) chloride tetrahydrate $MnCl_2\cdot4H_2O$) with 2,3,7,8,12,13,17,18-octaethylporphyrin in boiling dimethylformamide. The reaction mixture was diluted with an equal volume of water and extracted with chloroform. The extract was repeatedly washed with water to remove excess manganese salt and DMF. The product was identified and checked for purity by electronic and IR spectroscopy. Electronic absorption spectrum (toluene), λ_{max}, nm (logε): 359 (4.94), 428 (4.15), 473 (4.76), 562 (4.00), 591 (3.71), 677 (3.21), 770 (3.33). IR spectrum (KBr), ν, cm^{-1}: 2966, 2872 (CH_3); 2931 (CH_2); 1632, 1604 (C=C, C=N; 1480, 1464, 1451, 1373 (δCH_3, δCH_2); 1315 (C–N); 1272, 1148, 1112, 1062, 1019, 989, 962 (macrocycle); 1055 (δC_β–C); 841 (γC_{meso}–H); 749, 728 (γC_β–C). Mass spectrum (MALDI-TOF): *m*/*z* 587.43 [MnOEtPor]$^+$. $C_{36}H_{44}MnN_4$. Calculated: *M* 587.72.

2′-(Pyridin-4-yl)-5′-(pyridin-2-yl)-1′-(pyridin-3-ylmethyl)-2′,5′-dihydro-1′*H*-pyrrolo[3′,4′:1,9]-(C_{60}-I_h)[5,6]fullerene (Py_3C_{60}) was synthesized from C_{60} and the corresponding azomethine ylide[1] [27] in 1,2-dichlorobenzene. Electronic absorption spectrum (toluene), λ_{max}, nm (logε): 294, 313, 433 (3.82). IR spectrum (KBr), ν, cm^{-1}: 1721, 1689, 1636, 1587, 1572, 1455, 1426, 1377, 1356, 1307, 1279, 1231, 1215, 1187, 1157, 1123, 1096, 1064, 1048, 1026, 996, 962, 876, 845, 824, 799, 748, 711, 672, 627, 599, 574, 548, 527, 481, 399.

Pyridine of analytical grade was dried for 48 h over KOH pellets and distilled (bp 115.3°C). Toluene was dried over potassium hydroxide and distilled prior to use (bp 110.6°C). Water content was determined by Karl Fisher titration; it did not exceed 0.01%.

The reaction of (Cl)MnOEtPor with pyridine in toluene was studied by spectrophotometry at 298–318 K. A series of solutions with a constant concentration of (Cl)MnOEtPor (10^{-5} M) and different concentrations of pyridine (0–7 M) were prepared. The equilibrium constant *K* was determined by Eq. (2) for a three-component system with two colored components; the data were processed by the least-squares method implemented in Microsoft Excel.

$$K = \frac{\dfrac{A_i - A_0}{A_\infty - A_0}}{1 - \dfrac{A_i - A_0}{A_\infty - A_0}} \cdot \frac{1}{\left(c_{Py} - c^0_{(Cl)MnOEtPor}\dfrac{A_i - A_0}{A_\infty - A_0}\right)^n}. \qquad (2)$$

Here, c_{Py} and $c^0_{(Cl)MnOEtPor}$ are the initial concentrations of pyridine and (Cl)MnOEtPor, respectively, and A_0, A_i, and A_∞ are the optical densities at λ 360 nm of (Cl)MnOEtPor, equilibrium mixture at a definite pyridine concentration, and product, respectively. The relative error in the determination of *K* did not exceed 15%. The stoichiometric coefficient *n* was determined as the slope of the straight line $\log I_i = f(\log c_{Py})$, where

$$I_i = (A_i - A_0)/(A_\infty - A_i).$$

The kinetics of the reaction of (Cl)MnOEtPor with Py_3C_{60} in toluene were studied by spectrophotometry under pseudofirst-order conditions at 298 K (Py_3C_{60} concentration 0–1.5×10^{-4} M). The upper limit of the

[1] Provided by Prof. P.A. Troshin.

Py_3C_{60} concentration was determined by its solubility in toluene. Solutions of (Cl)MnOEtPor and Py_3C_{60} in freshly distilled toluene were prepared just before use to avoid peroxide formation. The optical densities of a series of solutions with a constant concentration of (Cl)MnOEtPor (1.0×10^{-5} M) and different Py_3C_{60} concentrations were measured at λ 475 nm immediately after mixing the reactants and after a time. The spectra were recorded relative to a solution of Py_3C_{60} with the same concentration. Solutions were maintained at 298±0.1 K in closed quartz cells. The rate constants for the reaction of (Cl)MnOEtPor with Py_3C_{60} were calculated assuming first-order kinetics (excess Py_3C_{60}):

$$k_{ef} = 1/\tau \ln[(A_0 - A_\infty)/(A_\tau - A_\infty)].$$

Here, A_0, A_τ, and A_∞ are the optical densities of the reaction mixture at a working wavelength at the initial moment, after time τ, and after reaction completion.

Quantum chemical calculations (PM3) [28–30] of isolated (Cl)MnOEtPor molecule and its complex with pyridine were performed with full geometry optimization until a gradient of 0.001 kJ mol^{-1} $Å^{-1}$. The averaged bond lengths and bond angles given in [31] were used as initial geometric parameters.

This study was performed under financial support by the Russian Foundation for Basic Research (project no. 15-43-03013-r-tsentr-a) using the facilities of the Upper Volga Joint Regional Center for Physicochemical Studies.

REFERENCES

1. Overbye, K.M. and Barrett, J.F., *Drug Discovery Today*, 2005, vol. 10, p. 45.
2. Levy, S.B., *Adv. Drug. Delivery Rev*., 2005, vol. 57, p. 1446.
3. Alanis, A.J., *Arch. Med. Res*., 2005, vol. 36, p. 697.
4. Chopra, I., *Curr. Opin. Microbiol*., 1998, vol. 1, p. 495.
5. Spellberg, B., Powers, J.H., Brass, E.P., Miller, L.G., and Edwards, J.E., *Clin. Infect. Dis*., 2004, vol. 38, p. 1279.
6. Livermore, D.M., *Lancet Infect. Dis*., 2005, vol. 5, p. 450.
7. Tome, J.P., Neves, M.G., Tome, A.C., Cavaleiro, J.A., Soncin, M., Magaraggia, M., Ferro, S., and Jori, G., *J. Med. Chem*., 2004, vol. 47, p. 6649.
8. Branland, V.S.P., Chaleix, V., Granet, R., Guilloton, M., Lamarche, F., Verneuil, B., and Krausz, P., *Bioorg. Med. Chem. Lett*., 2004, vol. 14, p. 4207.
9. Banfi, S., Caruso, E., Buccafurni, L., Battini, V., Zazzaron, S., Barbieri, P., and Orlandi, V., *J. Photochem. Photobiol., B*, 2006, vol. 85, p. 28.
10. Huang, L., Dai, T., and Hamblin, M., *Meth. Mol. Biol*., 2010, vol. 635, p. 155.
11. Meloa, W., Leeb, A.N., Perussi, J.R., and Hamblin, M.R., *Photodiagn. Photodyn. Ther.*, 2013, vol. 10, p. 647.
12. Lopes, M., Alves, C.T., Raju, B.R., Gonçalves, M.S.T., Coutinho, P.J.G., Henriques, M., and Belo, I., *J. Photochem. Photobiol., B*, 2014, vol. 141, p. 93.
13. Dukhande, V.V., Malthankar-Phatak, G.H., Hugus, J.J., Daniels, C.K., and Lai, J.C.K., *Neurochem. Res*., 2006, vol. 31, p. 1349.
14. Xiang-Jiao, X., Zhi, X., Zu-De, Q., An-Xin, H., Chao-Hong, L., and Yi, L., *Thermochim. Acta*, 2008, vol. 476, p. 33.
15. Karimipour, G., Kowkabi, S., and Naghiha, A., *Braz. Arch. Biol. Technol*., 2015, vol. 58, p. 431.
16. Spesia, B., Milanesio, M.E., and Durantini, E.N., *Eur. J. Med. Chem*., 2008, vol. 43, p. 853.
17. Fedorova, E., Klimova, R.R., Tulenev, Yu.A., Chichev, E.V., Kornev, A.B., Troshin, P.A., and Kushch, A.A., *Mendeleev Commun*., 2012, vol. 22, p. 254.
18. Zaitseva, S.V., Zdanovich, S.A., and Koifman, O.I., *Russ. J. Gen. Chem*., 2013, vol. 83, p. 738.
19. Klyueva, M.E., *Doctoral (Chem.) Dissertation*, Ivanovo, 2006.
20. Vinogradskii, A.G. and Sidorov, A.N., *Koord. Khim*., 1979, vol. 5, p. 800.
21. Ovchenkova, E.N., Bichan, N.G., and Lomova, T.N., *Tetrahedron*, 2015, vol. 71, p. 6659.
22. Razumov, V.F., Abalyaeva, V.V., and Efimov, O.N., *Nanostrukturirovannye materialy dlya zapasaniya i preobrazovaniya energii* (Nanostructured Materials for Energy Storage and Conversion). Ivanovo: Ivanov. Gos. Univ., 2009.
23. Lomova, T.N., Malov, M.E., Klyuev, M.V., and Troshin, P.A., *Macroheterocycles*, 2009, vol. 2, p. 164.
24. Lomova, T.N., Malov, M.E., Klyuev, M.V., and Troshin, P.A., *Advances in Materials Science Research*, Wythers, M.C., Ed., New York: Nova Science, 2011, vol. 2, p. 143.
25. Eletskii, A.V. and Smirnov, B.M., *Phys.–Usp*., 1993, vol. 36, p. 202.
26. Adler, A.D., Longo, F.R., Kampus, F., and Kim, J., *J. Inorg. Nucl. Chem*., 1970, vol. 32, p. 2443.
27. Troshin, P.A., Troyanov, S.I., Boiko, G.N., Lyubovskaya, R.N., Lapshin, A.N., and Goldshleger, N.F., *Fullerenes, Nanotubes, Carbon Nanostruct*., 2004, vol. 12, p. 435.
28. Stewart, J.J.P., *J. Comput. Chem*., 1989, vol. 10, p. 209.
29. Stewart, J.J.P., *J. Comput. Chem*., 1989, vol. 10, p. 221.
30. Stewart, J.J.P., *J. Comput.-Aided Mol. Des*., 1990, vol. 4, p. 1.
31. Lomova, T.N. and Berezin, B.D., *Russ. J. Coord. Chem*., 2001, vol. 27, p. 85.